EXISTENCE OF ASYMPTOTIC SOLUTIONS TO SEMILINEAR PARTIAL DIFFERENCE EQUATIONS ON GRAPHS
A RESEARCH EXPERIENCE FOR UNDERGRADUATES REPORT, NORTHERN ARIZONA UNIVERSITY, 2007.

REU: JASON D. LEE AND MENTOR: JOHN NEUBERGER

Abstract. This paper studies nonlinear partial difference equations on graphs. We seek solutions to the semilinear equation $-Lu + su + u^3 = 0$ where L is the Laplacian of a graph $G = (V, E)$. In particular we prove the existence of 3^n solutions when $s \to -\infty$ and $n = |V|$. In addition, we find their Morse indices and exact forms. In [4], the authors used the tGNGA method to produce bifurcation diagrams for several graphs; however, these diagrams are not complete. This study complements [4] by using the asymptotic solutions to construct a complete bifurcation diagram.

1. Introduction

This paper studies nonlinear elliptic partial difference equations. In particular we investigate asymptotic solutions and determine their relationship to the Nehari manifold. Partial difference equations are discretized versions of partial differential equations and arise whenever the finite differences technique is used to numerically solve a PDE. Finite differences introduces a grid and that grid can be considered a simple connected graph. The Laplacian operator is then replaced by the discrete Laplacian operator. We concentrate on using the Laplacian matrix of the graph which is an unscaled discrete Laplace operator. Our main result is illustrated using numerical simulations for graphs with a small number of vertices, but holds true for any graph or grid. It is also expected that after proper scaling of the Laplacian matrix that studying partial difference equations leads directly to new knowledge of nonlinear elliptic equations with both Neumann and Dirichlet boundary conditions. We discuss the

2000 *Mathematics Subject Classification.* Primary 58J37, 35A05; Secondary 35A15, 58J55,05C50.

Key words and phrases. Semilinear Elliptic Equations, Semilinear Elliptic Systems, Difference Equations, Nehari Manifold, Bifurcations,Asymptotic.

This research was supported by an NSF REU grant to Northern Arizona University.

connection between partial difference equations and partial differential equations (PDE) and possible implications of our results and numerical simulations to PDEs. (the stuff below is not actually discussed) Also we determine the exact solutions for an ODE with Neumann boundary conditions and discuss the similarities with the partial difference equations on P_n, the path graph on n vertices. We also highlight the similarities between the ODE with periodic boundary conditions and partial difference equations on C_n, the cycle graph on n vertices. For our numerical studies we restrict ourselves to semilinear elliptic equations and odd nonlinearities, but our analysis could be applied to more general nonlinearities without much difficulty. We note that our main result provides a way to find the complete bifurcation diagram for a class of semilinear elliptic partial difference equations using the GNGA algorithm of Neuberger, Sieben and Swift described in [4] and possibly paves way to a new proof of an infinite number of solutions to semilinear elliptic equations with even action functionals.

2. Preliminaries

We are interested in solving semilinear elliptic partial differential equations of the form

$$\begin{aligned} \Delta u + f(u) = 0 \quad u \text{ in } \Omega \\ \frac{\partial u}{\partial \eta} = 0 \text{ in } \partial\Omega, \end{aligned} \tag{2.1}$$

where f is subcritical, superlinear and $f(0) = 0$. The exact restrictions on f can be found in [1] and [2].
The corresponding partial difference equation is

$$-Lu + f(u) = 0 \tag{2.2}$$

where L denotes the Laplacian matrix of a simple undirected connected graph G. Let $G = (V, E)$ be a simple connected graph with $m = |V|$ and $n = |E|$. Then the Laplacian matrix, $L(G)$ is an $m \times m$ matrix with $L_{jj} = d_j$ where d_j denotes the degree of the $j - th$ vertice and $L_{ij} = -1$ if $(v_i, v_j) \in E$ and $L_{ij} = 0$ otherwise. D, the edge incidence matrix of a graph or first order difference operator, is an $n \times m$ matrix where for each edge $e_k = (v_i, v_j)$ we have $D_{ki} = -1$ and $D_{kj} = 1$. The edge-incidence matrix and Laplacian matrix are connected by the equation $D^T D = L$.

We now list several useful properties of L.

1. L has no nonnegative eigenvalues with a simple eigenvalue $\lambda_1 = 0$ and ϕ_1 can be taken as $\phi_1 = (1, 1, \ldots, 1, 1)$ L has all positive eigenvalues with $\lambda_1 = 0$ with first eigenvector $\phi_1 = (1, 1, \ldots, 1, 1)$.

2. $Lu \cdot u = \sum_{(i,v)\in E(G)}^{k=m} (u(i) - u(j))^2$

Equation (2.1) has a variational formulation and is associated with the action functional $J : H_0^{1,2}(\Omega) \to \mathbb{R}$

$$\begin{aligned} J(u) &= \int_\Omega (\frac{|\nabla u|^2}{2} - F(u)) \\ F(u) &= \int f(u) \end{aligned} \tag{2.3}$$

If the nonlinearity f is subcritical and satisfies the additional restrictions in [1] then it has been shown that $J(u)$ is twice differentiable and weak solutions of (2.3), $u \in H$ that satisfy

$$J'(u)(v) = \int_\Omega (\nabla u \cdot \nabla v - f(u) \cdot v) = 0 \tag{2.4}$$

for all $v \in H$ are also solutions to (2.1).
We now proceed to construct an analagous variational formulation to (2.2). Let $J : \mathbb{R}^n \to \mathbb{R}$ be defined as

$$J(u) = \frac{1}{2} Du \cdot Du - \sum_{i=1}^{m} F(u_i) \tag{2.5}$$

where D is the first order difference matrix associated to the graph or else known as the edge-incidence matrix of a graph. We take u^2 to mean $u^2 = (u_1^2, \ldots, u_m^2)$.
We now follow [1] and [2] to define a finite dimensional analogue of the Nehari Manifold.

$$S = \{u \in \mathbb{R}^m - \{0\} : J'(u)(u) = 0\} \tag{2.6}$$

The following list of properties of the Nehari Manifold S is taken from [3].

1. S is a $(m-1)$-dimensional manifold in $\mathbb{R}^m$ and is diffeomorphic to $\mathbb{S}^{m-1}$ when $f'(0) < \lambda_1$. Otherwise S is degenerate and not a manifold.
2. S is compact unlike in the infinite dimensional case.
3. $\forall u \neq 0 \in \mathbb{R}^m$ there exists a unique $t > 0$ such that $tu \in S$
4. For all $u \in S$, $J(u) \geq J(\alpha u)$ for all $\alpha \in [0, \infty)$.
5. The Nehari Manifold is a natural constraint. u is a nontrivial solution iff u is a critical point of $J|_s$.
6. J is bounded above on S.

In [1] it was shown that (2.1) has 2 nontrivial, non sign-changing solutions when $f'(0) < \lambda_1$ where λ_1 denotes smallest eigenvalue of Δ. Furthermore [2] used a modified mountain pass theorem and proved that there exists a third

solution that is Morse Index 2 and exactly once sign-changing.
In [3], the author adapted the mountain pass theorem of Ambrosetti-Rabinowitz to show that (2.2) has 2 one sign solutions and 1 Morse Index 2 exactly once sign-changing solution. In the partial difference equation case, $f(u)$ only needs to be superlinear, $f'(u) > \frac{f(u)}{u}$, and $f(0) = 0$. The subcritical restriction and coercivity condition are unneccesary in this case.

In Section 3 we state an existence theorem to (2.2) for a certain class of $f(u)$.

3. Bifurcation Diagrams

In this section, we compare 2 different methods of drawing the bifurcation diagram for the difference equation $-Lu + su + u^3$. A bifurcation diagram plots the parameter s on the x-axis and $N(u) : \mathbb{R}^m \to \mathbb{R}$ on the y-axis. $N(u)$ is usually a norm of u or $J(u)$. For our numerical experiments we let $N(u)$ be the taxicab norm. Figure (2) is an example of a bifurcation diagram. In [4], the authors developed the GNGA suite of algorithms to construct bifurcation diagrams for the partial difference equation $-Lu + f(u) = 0$ and $f_s(u) = su + u^3$, where $s = f'(0)$ is a parameter. We also develop the Asymptotic Branch Following method (ABF) and compare the resulting bifurcation diagrams with those made using the algorithm of Neuberger, Sieben and Swift (NSS).

3.1. GNGA.

This section reviews the GNGA algorithm of Neuberger, Sieben and Swift (NSS) outlined in [4]. We assume that $u = \sum_{i=1}^{m} c_i \psi_i$ and seek coefficients $c \in \mathbb{R}^m$ such that the coefficient vector of the standard gradient's eigenfunction expansion $g_i = J'(u)(\psi_i)_{i=1,\dots,m}$ is zero. Such coefficient vectors are solutions since $J'(u)(v) = 0$ for all v. The gradient is defined as

$$g_i = c_i \lambda_i - f(u) \cdot \psi_i \tag{3.1}$$

Similarly, the Hessian h defined by $h = (J''(u)(\psi_i, \psi_j))_{i,j=1,\dots,m}$ and can be computed as

$$h_{ij} = \lambda_i \delta_{ij} - f'(u)\psi_i \cdot \psi_j \tag{3.2}$$

Applying Newton's method to find zeros of g results in the GNGA algorithm:

1. Initialize $c = c^0 \in \mathbb{R}^m$ and set $= u^0 = \sum c_i \psi_i$
2. Loop until $||g||$ is sufficiently small
   (a) Compute g
   (b) Compute h
   (c) Solve for Newton step direction χ that satisfies $h\chi = g$.
   (d) Take a Newton step. $c^{k+1} = c^k - \chi$
   (e) Compute new g and check if it is sufficiently small.
3. Output data to be plotted on a bifurcation diagram.

The output data can vary depending on the experiment, but typical choices are $||u||$, the taxicab norm of u, $J(u)$, and the signature sig(u) which is equal to the Morse Index if u is a solution. The MI can be thought of as the number of down directions of u, e.g., $MI = 0$ for maxima, $MI = m$ for maxima and $MI \in 1, \ldots, m-1$ for saddle points. The search direction χ, is solved for using any linear solver algorithm and noninvertible hessians will occur at bifurcation points.

3.2. **Newton's Method with Constraints.** To follow branches, it is necessary to treat the parameter s as the $(m+1)^{\text{st}}$ unknown. Thus, when we say $(a, s) \in \mathbb{R}^{m+1}$ is a solution, we mean that $u = \sum a_i \psi_i$ solves (2.1) with parameter s. We restrict the search for a particular solution (a, s) to some hypersurface in $\mathbb{R}^{m+1}$, satisfying an $(m+1)^{\text{st}}$ equation of the form $\kappa(a, s) = 0$. We take either a pair of known solutions along a symmetry invariant branch or take a solution known to be a bifurcation point together with knowledge of the corresponding critical eigenspace to obtain a reasonable initial guess $(a, s)_0$ for iterating to find a nearby solution satisfying the constraint. The iteration we use is:

- Compute the auxillary constraint κ, gradient vector $g := g_s(u)$, and Hessian matrix $h := h_s(u)$
- Solve $\begin{bmatrix} h & \frac{\partial g}{\partial s} \\ \nabla_a \kappa & \frac{\partial \kappa}{\partial s} \end{bmatrix} \begin{bmatrix} \chi_a \\ \chi_s \end{bmatrix} = \begin{bmatrix} g \\ \kappa \end{bmatrix}$
- $(a, s) \leftarrow (a, s) - \delta\chi, \quad u = \sum a_i \psi_i.$

The $(m+1)^{\text{st}}$ row of the matrix is defined by $(\nabla_a \kappa, \frac{\partial \kappa}{\partial s}) = \nabla\kappa \in \mathbb{R}^{m+1}$; for appearance the search direction χ can be likewise partitioned as $\chi = (\chi_a, \chi_s) \in \mathbb{R}^{m+1}$. Since this is Newton's method on $(g, \kappa) \in \mathbb{R}^{m+1}$ instead of just $g \in \mathbb{R}^m$, when the process converges we have not only that $g = 0$ (hence (u, s) is a solution to (2.1)), but also that $\kappa = 0$ (so that u belongs to the constrained set).

3.3. **tGNGA.** The Newton's method with Constraints is referred to as the Tangent Augmented Gradient Newton Galerkin Algorithm(tGNGA) in [4]. When following a branch we use the two previously found solutions $(\tilde{a}, \tilde{s})$ and $(\tilde{\tilde{a}}, \tilde{\tilde{s}})$ lying on that branch. With the normalized approximate tangent vector $v = ((\tilde{a}, \tilde{s}) - (\tilde{\tilde{a}}, \tilde{\tilde{s}}))/||(\tilde{a}, \tilde{s}) - (\tilde{\tilde{a}}, \tilde{\tilde{s}})|| \in \mathbb{R}^{m+1}$ we obtain the initial guess $(a_0, s_0) = (\tilde{a}, \tilde{s}) + cv$. In our experiments it has sufficed to fix the speed c, for example, .2 or .4, but this value can be chosen dynamically according to the scale and complexity of features, e.g., severe turning points or proliferation of proximal bifurcation points on the branch. For tGNGA, the constraint is that the i^{th} iterate (a_i, s_i) must lie on the hyperplane passing through the initial guess $(a, s)_0$, perpendicular to v. That is, $\kappa(a, s) := ((a, s) - (a_0, s_0)) \cdot v$. Easily, one sees that $(\nabla_a \kappa(a, s), \frac{\partial \kappa}{\partial s}(a, s)) = v$ and that $g_s(a) = (a_j(\lambda_j - s) -$

$(\sum_i^m a_i\psi_i)^3 \cdot \psi_j))_{j=1}^m$ implies $\frac{\partial g}{\partial s} = -a$. Newton's method is invariant in this plane so that in fact $\chi \cdot v = 0$ at each step. Hence, the linear system to be solved each iteration can be described by:

$$\begin{bmatrix} h & -a \\ v_a & v_s \end{bmatrix} \begin{bmatrix} \chi_a \\ \chi_s \end{bmatrix} = \begin{bmatrix} g \\ 0 \end{bmatrix},$$

where again for appearance $v = (v_a, v_s) \in \mathbb{R}^{n+1}$ can be partitoned into 2 components.

3.4. **Branch Following of Asymptotic Solutions.** In the previous section we showed that $-Lu + su + u^3 = 0$ must have 3^m asymptotic solutions. Thus we begin following each solution at a large negative s paramter. Experimentation shows that $s = -10$ is sufficiently large that initial guesses of the form $u_k = \sqrt{-s}$ or 0 converge by Newton's method. For each solution we use the Asymptotic Branch Following method.

3.5. **Asymptotic Branch Following (ABF).**

1. Set initial guess u^0 to an asymptotic solution with $u_k = \pm\sqrt{-s_0}$ or 0. Run GNGA with u^0 as initial guess and store solution as u^0
2. Let $s_1 = s_0 + \epsilon$ and run GNGA with u^1 as initial guess with $u_k = \pm\sqrt{-s_1}$ or 0. Store solution in u^1.
3. Use u^1 and u^0 as the 2 initial points for tGNGA method and use tGNGA to follow the branch.
4. Repeat for each asymptotic solution.

3.6. **Comparison of Asymptotic Branch Following (ABF) and NSS methods.** The implementation in [4] is described in detail but we give a brief overview

1. Uses the tGNGA method to follow the trivial branch $u \equiv 0$. Finds places where Morse Index changes since these are bifurcation points or turning points.
2. Finds a new solution point off of the trivial branch then uses the tGNGA method to follow those branches. Repeats process until no more bifurcation points are found.

This method will find all branches connected to $u \equiv 0$, but misses those that are not connected to the trivial branch. The authors of [4] hoped that all branches were connected to the trivial branch but now with ABF we can test that hypothesis since ABF will find all branches.

The only difference between ABF and NSS is the initial guesses. NSS uses the trivial initial guess $u \equiv 0$. Asymptotic Branch Following(ABF) uses a more intelligent initial guess based on the known asymptotic solutions. Beyond that, the two algorithms both utilize the tGNGA branch following algorithm. We

FIGURE 1. Path Graph on 3 vertices, also known as P3

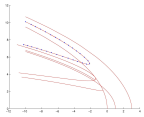

FIGURE 2. Bifurcation Diagram for P3 using Asymptotic Solutions. The branch with blue points is not found by the NSS method of [4]

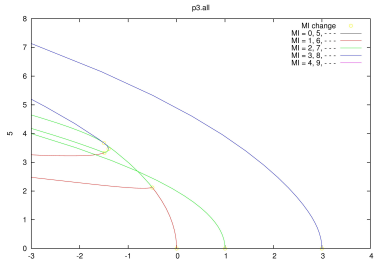

FIGURE 3. Bifurcation Diagram for P3 using NSS. This diagram is missing a branch that Figure (2) has.

now compare the bifurcation diagrams constructed using ABF and NSS for P3.

Figures (2) and (3) are identical except that Figure (2) has the extra branch labelled with blue dots. Although this branch intersects a branch connected to the trivial branch $u \equiv 0$, it is not connected. The intersection is due to the choice of norm. The ABF method finds this since it follows the asymptotic solutions. In fact, the ABF method will find all solutions since the equation $-Lu + su + u^3 = 0$ has at most 3^m solutions and since we are following 3^m the bifurcation diagram constructed using ABF is complete. We see the same phenomenon of ABF finding a branch that NSS fails to find in the Figures (4) and (5).

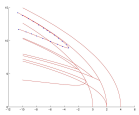

FIGURE 4. Bifurcation Diagram for C4 using Asymptotic Solutions. The branch with blue points is not found by the NSS method of [4]

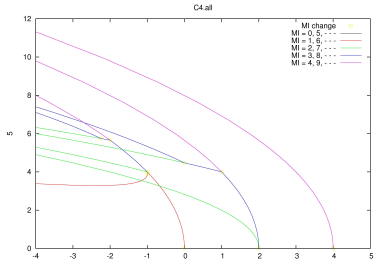

FIGURE 5. Bifurcation Diagram for C4 using GNGA. This diagram is missing a branch that Figure (4) has.

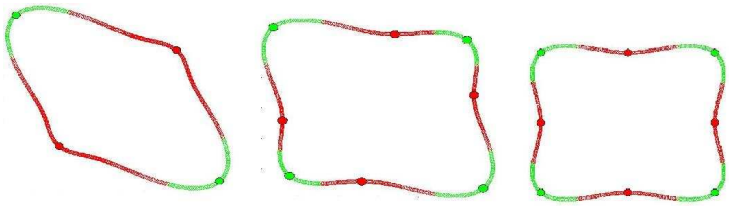

FIGURE 6. The Nehari Manifold for K2 at s=-1, -5 and -100

4. Nehari Manifold

We look at the Nehari Manifold associated with the equation $-Lu + su + u^3 = 0$ for various graphs and values of s. First we look at the Nehari Manifold for K2, the complete graph on 2 vertices. The Nehari Manifold for K2 is homeomorphic to a circle when $s < 0$ but equation 2.2 has different numbers of unique solutions for different values of s. Figure 6 shows the Nehari Manifold at $s = -1, -5, -100$ and the green circles are solutions of Morse Index 1 and the red circles are solutions of Morse Index 2. At $s = -1$, the equation only has 5 solutions($u = 0$ solution is not displayed) but for $s = -5$ and -100 it has $3^2 = 9$ solutions. This is a general trend seen in all graphs; the number of solutions to 2.2 increases as the parameter s decreases. Also the Nehari Manifold tends towards a square shape for $s \to -\infty$ and the solutions are the edges and faces of the square (see last diagram of Figure 6).

The Nehari Manifold for K3(Figure 7) and P3(Figure 8 exhibit similar behavior. More solutions appear as s decreases and it achieves the maximum of $3^3 = 27$ solutions at $s = -100$. Furthermore, the solutions at $s = -100$ lie on the vertices, edges and faces of a 3-cube meaning $u = \sqrt{-s} \cdot (1, 1, 1), \sqrt{-s} \cdot (1, 0, 1)$ and so on are all solutions as $s \to -\infty$.

Another observation is that the solutions at $s = -100$ does not depend on the specific graph, that is K3 and P3 have almost the same solutions as $s = -100$. This is seen in Figure 9 by comparing the Nehari Manifolds for K3 and P3 at a large negative value of s. This indicates that the asymptotic solutions are independent of the graph and for a n-vertex graph, the solutions are always the vertices, edges, and faces of an n-cube.

However at $s = -1$, the Nehari Manifold and solutions to Equation 2.2 for P3 and K3 are very different. Figure 10 shows the Nehari Manifold for K3 and P3 at $s = -1$. The Nehari Manifolds for these 2 graphs are different and the solutions are different. This can also be seen by comparing the bifurcation diagrams for K3 and P3 in Figures 11 and 12. From the bifurcation diagrams, it is clear that the solutions for K3 and P3 are different , but for large negative values of s we start to see some clumping of solutions towards 3 particular

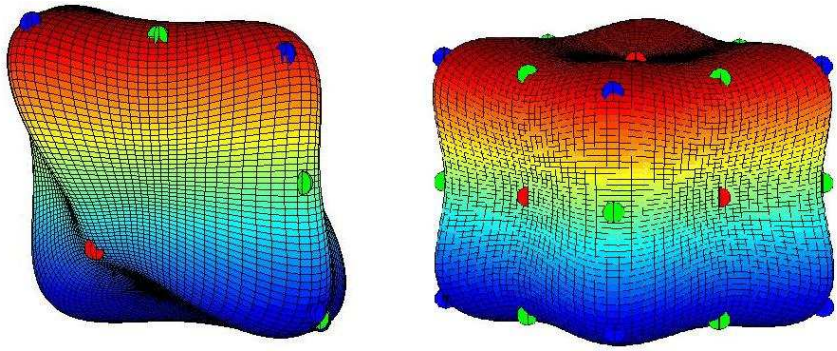

FIGURE 7. The Nehari Manifold for K3 at $s = -1$ and $s = -100$

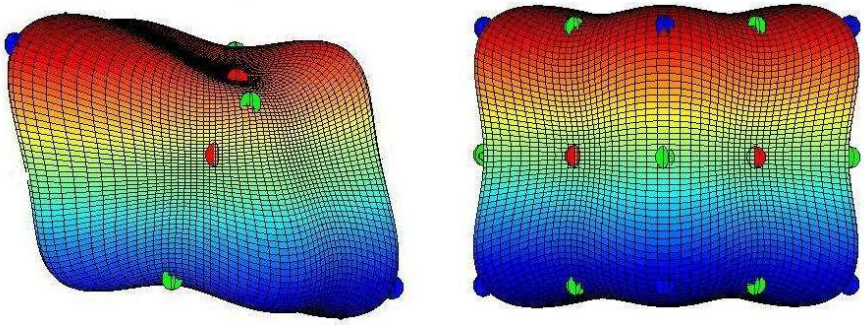

FIGURE 8. The Nehari Manifold for P3 at $s = -1$ and $s = -100$

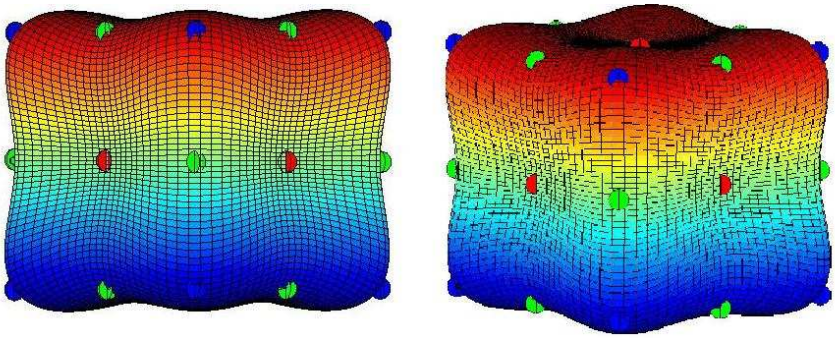

FIGURE 9. The Nehari Manifold for P3 and K3 at $s = -100$

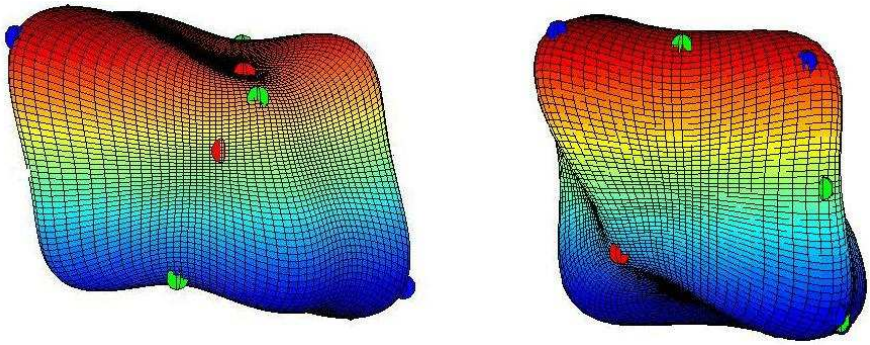

FIGURE 10. Nehari Manifold for P3 and K3 at $s = -1$

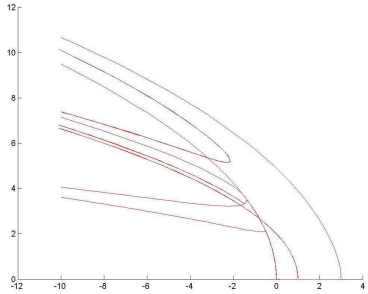

FIGURE 11. Bifurcation Diagram for P3

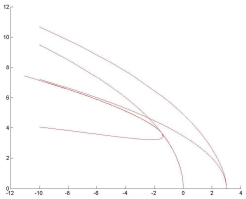

FIGURE 12. Bifurcation Diagram for K3

values. For K3 and P3 at $s = -10$, the norms clump to $3 * \sqrt{10}$, $2 * \sqrt{10}$ and $\sqrt{10}$. In the next section, we formalize these observations of the Nehari Manifold and the solutions to all graphs.

5. Results

Theorem 5.1 (Asymptotic Solutions)**.**
On a graph of m vertices, Newton's method will find 3^m solutions to the equation $-Lu + su + |u| \cdot u^{p-1} = 0$ when $s \to -\infty$.

Corollary 1 (Exact Asymptotic Solutions)**.**
The solutions found by Newton's Method are

$$u = (-s)^{\frac{1}{p-1}} \cdot (j_1, j_2, \ldots, j_m) \text{ and } j_k = 0 \text{ or } \pm 1. \tag{5.1}$$

when $s \to -\infty$.

Corollary 2 (Morse Indices of Asymptotic Solutions)**.**
Of the solutions found by Newton's method as $s \to -\infty$, there will be $2^{m-k} \cdot \binom{m}{k}$ solutions of Morse Index $(m-k)$ where m denotes the number of vertices and k denotes the number of l where $j_l = 0$ in the solution.

6. Proofs

We now prove Theorem (5.1) and Corollaries (1) and (2).

Proof. We will show that $J'(u)(v) \to 0$ as $s \to -\infty$ for the u given in Corollary (1), so Newton's method will recognize these as critical points. The definitions of the $J(u)$ and $J'(u)(v)$ functionals are

$$\begin{aligned} J'(u)(v) &= -(-Lu + su + |u| \cdot u^{p-1}) \cdot v = 0 \text{ for all } v \in \mathbb{R}^m \\ J(u) &= \frac{1}{2} Lu \cdot u - \frac{su \cdot u}{2} - \sum_{i=1}^{i=m} \frac{|u|^{p+1}}{p+1} \end{aligned} \tag{6.1}$$

It is clear that u_0 is a critical point of J iff

$$\lim_{\delta \to 0} \frac{J(u_0 + \delta e_j) - J(u_0)}{\delta} = 0 \tag{6.2}$$

for all e_j, where e_j are the standard unit vectors in $\mathbb{R}^m$. This condition is equivalent to $J'(u_0)(v) = 0$ for all $v \in \mathbb{R}^m$. Now we will show that when u is defined as in Corollary (1) then $J'(u)(v) \to 0$ as $s \to -\infty$ for all v. Consider $u = (j_1, \ldots, j_m)$ where $j_k = (0 \text{ or } \pm 1)$ and $u' = u_0 + \delta \cdot e_k$.

$$\begin{aligned} J(u') - J(u) &= \frac{1}{2} Lu' \cdot u' - \frac{1}{2} Lu \cdot u - \frac{su' \cdot u'}{2} + \frac{su \cdot u}{2} - \sum_{j=1}^{j=m} \left(\frac{|u_j|^{p+1} - |u'_j|^{p+1}}{p+1}\right) \\ &= \frac{1}{2} \sum_{\substack{(i,k) \in E(G) \\ i=1}}^{i=m} [(u_k - u'_i)^2 - (u_k - u_i)^2] - \frac{su' \cdot u'}{2} + \frac{su \cdot u}{2} - \sum_{j=1}^{j=m} \left(\frac{|u_j|^{p+1} - |u'_j|^{p+1}}{p+1}\right) \\ &= \frac{1}{2} \sum_{\substack{(i,k) \in E(G) \\ i=1}}^{i=m} [2\delta(u_k - u_i) + \delta^2)] - \frac{su' \cdot u'}{2} + \frac{su \cdot u}{2} - \sum_{j=1}^{j=m} \left(\frac{|u_j|^{p+1} - |u'_j|^{p+1}}{p+1}\right) \\ &= \sum_{\substack{(i,k) \in E(G) \\ i=1}}^{i=m} [\delta(u_k - u_i) + \frac{\delta^2}{2}] - \frac{su' \cdot u'}{2} + \frac{su \cdot u}{2} - \sum_{j=1}^{j=m} \left(\frac{|u_j|^{p+1} - |u'_j|^{p+1}}{p+1}\right) \end{aligned}$$

Since $u'_j = u_j$ for all $j \neq k$ we can remove the summation and simplify the dot product.

$$= \sum_{\substack{(i,k)\in E(G)\\ i=1}}^{i=m} [\delta(u_k - u_i) + \frac{\delta^2}{2}] + \frac{su_k \cdot u_k}{2} - \frac{su'_k \cdot u'_k}{2}$$
$$+ \frac{|u_k|^{p+1}}{p+1} - \frac{|u'_k|^{p+1}}{p+1}$$

Case 1: $u_k = 0$ and $u'_k = \delta$

$$|J(u') - J(u)| = |\sum_{\substack{(k,i)\in E(G)\\ i=1}}^{i=m} [-u_i\delta + \frac{\delta^2}{2}] - \frac{\delta^2 s}{2} - \frac{\delta^{p+1}}{p+1}|$$
$$\leq ||d_k\delta(-s)^{\frac{1}{p-1}} + \frac{\delta^2}{2}| - \frac{\delta^2 s}{2} - \frac{\delta^{p+1}}{p+1}|$$

where d_k denotes the degree of the k-th vertex. For $s < s_0 = -(\frac{d_k}{\delta})^{\frac{p-1}{p-2}}$,

$$|J(u') - J(u)| \leq ||d_k[\delta(-s)^{\frac{1}{p-1}} + \frac{\delta^2}{2}]| - \frac{\delta^2 s}{2} - \frac{\delta^{p+1}}{p+1}|$$
$$\leq || - \frac{3}{2}s\delta^2| + \frac{d_k\delta^2}{2} - \frac{\delta^{p+1}}{p+1}|$$

From this, we see that $\lim_{\delta\to 0} |\frac{J(u') - J(u)}{\delta}| \leq ||\frac{-3}{2}s\delta| + \frac{d_k\delta}{2} - \frac{\delta^p}{p+1}| = 0$.

Case 2: $u_l = (-s)^{\frac{1}{p-1}}$

$$|J(u') - J(u)| = |\sum_{\substack{(k,i)\in E(G)\\ i=1}}^{i=m} [\delta((-s)^{\frac{1}{p-1}} - u_i) + \frac{\delta^2}{2}] - s(-s)^{\frac{1}{p-1}}\delta - \frac{\delta^2 s}{2}$$
$$- \frac{1}{p+1}((p+1)(-s)(-s)^{\frac{1}{p-1}}\delta + \binom{p+1}{2}\delta^2(-s) + O(\delta^3))|$$
$$= |\sum_{\substack{(k,i)\in E(G)\\ i=1}}^{i=m} [\delta((-s)^{\frac{1}{p-1}} - u_i) + \frac{\delta^2}{2}] - \frac{\delta^2 s}{2} - \frac{1}{p+1}(\binom{p+1}{2}\delta^2(-s) + O(\delta^3))|$$
$$\leq ||2d_k\delta(-s)^{\frac{1}{p-1}} + \frac{d_k\delta^2}{2}| - \frac{\delta^2 s}{2} - \frac{1}{p+1}(\binom{p+1}{2}\delta^2(-s) + O(\delta^3))|$$

For $s < s_0 = -(\frac{d_k}{\delta})^{\frac{p-1}{p-2}}$

$$|J(u') - J(u)| \leq ||2d_k\delta(-s)^{\frac{1}{p-1}} + \frac{d_k\delta^2}{2}| - \frac{\delta^2 s}{2} - \frac{1}{p+1}(\binom{p+1}{2}\delta^2(-s) + O(\delta^3))|$$

$$\leq ||\frac{-5}{2}s\delta^2| + \frac{d_k\delta^2}{2} - \frac{\delta^2 s}{2} - \frac{1}{p+1}(\binom{p+1}{2}\delta^2(-s) + O(\delta^3))|$$

From this we have,

$$\lim_{\delta\to 0}|\frac{J(u') - J(u)}{\delta}| \leq ||\frac{-5}{2}s\delta| + \frac{d_k\delta}{2} - \frac{\delta s}{2} - \frac{1}{p+1}(\binom{p+1}{2}\delta(-s) + O(\delta^2))| = 0$$

Since $J'(u)(v) \to 0$ as $s \to -\infty$ for all $v \in \mathbb{R}^m$, u will be recognized as a solution by Newton's Method. □

Proof. Now we will prove Corollary (2). This follows almost directly from the proof above. Consider an asymptotic solution $u = (u_1, u_2, u_3, \ldots, u_m)$. From Case 1 of the above proof we see that $J''(u)(e_k, e_k) > 0$ if $u_k = 0$ and from Case 2 we see that $J''(u)(e_k, e_k) < 0$ if $u_k = (-s)^{\frac{1}{p-1}}$. The Morse Index is equal to the number of e_k such that $J''(u)(e_k, e_k) > 0$. The Morse Index of the solution follows from counting the number of k such that $u_k = 0$. □

7. Conclusion and Future Research

Using the ABF method, we have managed to construct complete bifurcation diagrams for the model graph equation. These differ from those constructed using NSS in [4] and it is still unclear which branches will be connected to the trivial branch. For example, numerical experimentation shows that for the complete graphs K_m, all branches are connected to the trivial branch $u \equiv 0$. However, we find that for most other graphs, ABF finds disconnected branches that NSS will miss. Future studies should concentrate on which branches are connected to the trivial branch and which are not. Since complete graphs are very symmetrical and seem to have only connected branches, we conjecture that more symmetrical branches (branches with larger stabilizer groups) are connected to the trivial branch. Also primary bifurcation branches are generally more symmetrical than secondary bifurcations and secondary bifurcation branches more symmetrical than tertiary branches and so on. Perhaps disconnected bifurcation branches are those with no symmetry or very small symmetry groups.

Another unanswered question is which of the asymptotic solutions are part of primary, secondary, tertiary, or disconnected branches. For example, it is known that the primary bifurcation from $\lambda_1 = 0$ leads to the asymptotic solution $u_k = (-s)^{\frac{p-1}{p}}$ for all k. A way to associate each asymptotic solution with each branch would provide a way to find a lower bound on a s_0 such that when

$s < s_0$ the difference equation $-Lu + su + u^3 = 0$ has 3^m solutions. We currently know that there must exist an s_0 for which this is true, but cannot show that there is a lower bound to s_0. Further study in this area could also lead to a more refined classification of bifurcation branches by there symmetry.

References

1. Antonio Ambrosetti and Paul H. Rabinowitz, *Dual variational methods in critical point theory and applications*, J. Functional Analysis **14** (1973), 349–381.
2. Alfonso Castro, Jorge Cossio, and John M. Neuberger, *A sign-changing solution for a superlinear Dirichlet problem*, Rocky Mountain J. Math. **27** (1997), no. 4, 1041–1053.
3. John M. Neuberger, *Nonlinear elliptic partial difference equations on graphs*, Experiment. Math. **15** (2006), no. 1, 91–107.
4. John M. Neuberger, Nándor Sieben, and James W. Swift, *Symmetry and automated branch following for a semilinear elliptic pde on a fractal region*, SIAM J. of Dynam. Sys. (to Appear, 2006).

E-mail address: jdl17@duke.edu,John.Neuberger@nau.edu

(Jason Lee) Department of Mathematics, Duke University, Durham, NC 27708, USA

(John Neuberger) Department of Mathematics and Statistics, Northern Arizona University PO Box 5717, Flagstaff, AZ 86011-5717, USA